Vol. 8(28), Apr. 2018, PP. 3807-3815

Contents list available at IJMEC

International Journal of Mechatronics, Electrical and Computer Technology (IJMEC)

Journal Homepage: www.aeuso.org

PISSN: 2411-6173 - EISSN: 2305-0543

Nonlinear Damper Design for a Vibration Isolation System

U.H. Diala[1, a], K. C. Okafor [2,b*] and C.C. Udeze[3,c]

[1]*Dept. of Automatic Control and Systems Engineering, University of Sheffield, Western Bank, Sheffield, S10 2TN, UK.*

[2]*Dept. of Mechatronics Engineering (Computer Systems and Software Development Option), Federal University of Technology, Owerri, Nigeria.*

[3]*Dept. of Electronic Engineering (Control Systems Option), University of Nigeria, Nsukka, Nigeria.*

***Corresponding Author's E-mail** [b*]: kennedy.okafor@futo.edu.ng*

Abstract

In this paper, vibration transmissibility of a single-degree-of-freedom (SDOF) for a mass-spring-damper system is presented. This is done with a linear damper having a configuration perpendicular to a linear vertical spring. The method is analyzed using a nonlinear frequency analysis approach. The concept of the output frequency response function (OFRF) is used to derive an explicit polynomial relationship between the system output response (relative displacement of the mass) and the nonlinear damping coefficient which is the parameter of interest. With the derived OFRF polynomial, various damping parameters were designed for desired output responses. Real-time experimental results are presented for the vibration isolation system validation with dampers orientated perpendicularly (at 90 degrees) to the linear spring. The experimental case studies are provided to demonstrate the new OFRF-based nonlinear system design and its significance in isolated vibration system applications. A force transmissibility graph showing the system output using both numerical and the OFRF methods are presented.

Keywords: *Vibration Transmissibility; Real-Time Experiments; Single-Degree-of-Freedom; Time-Frequency Signal Analysis; Damped Systems.*

1. Introduction

The study of vibration dynamics is very important in complex mechatronics designs [1] such as mass-spring system models involving damping control approach with positive acceleration, velocity and position feedback (PAVPF) scheme [2]. This is a recent effort applied in piezo-actuated nanopositioning system used to achieve high-bandwidth operation [2]. This is considered to have single model of vibration [1]. But, forced vibration of damped SDOF including linear spring systems presents vibration problems not only in mechatronics systems, but in general engineering structures such as response prediction in bridges, buildings, car suspension systems, electron microscopes. Efforts must be made to isolate the systems from vibrations. Generally, vibration isolation is the process of isolating an object or device from the impending source of vibrations in a reliable manner. In an objective sense, vibration is undesirable in engineering systems and housable spaces like rotating machines or suspenders [3]. The test for acceptable performance is the transmissibility *T*. In simple terms, Force transmissibility in vibration structures is the ratio of the output force on the foundation to the input excitation. If the ratio, *T* is greater than *1*, this

Article History:
Received Date: Jan. 04, 2018
Accepted Date: Apr. 05, 2018
Available Online: Apr. 15, 2018

indicates that default amplification and maximum amplification happens when forcing frequency (f_f) and natural frequency (f_n) of the system converges at a point *P*. The transmissibility *T* is used to compute the system compensation efficiency. When the *vibration* level is high, it can result in unacceptable noise level. This can also lead machine failure. Machine vibration is the primary source in this context. In the past, methods have been developed to prevent the compounding transfer of vibration to such systems.

However, it has been investigated in [3], [4] that a vibration isolation system in which a linear damper is orientated perpendicularly to a linear vertical spring can cause nonlinear dynamics within the isolation system. The geometrical inclination of the linear damper created a nonlinear effect and the system was analyzed for its benefits in vibration isolation. Consider Figure 1 depicting complex vibration isolation systems with a) machine system bolted to a rigid foundation, b) Support on isolation springs riveted on a rigid foundation c) machine system attached to an inertia block d) supported on isolation springs, but on a non-rigid foundation (such as a floor); or machine on isolation springs, seismic mass and second level of isolator springs. The machine system depicts a single degree of freedom in the vertical dimension. However, efforts have been made in suspending the machine system without the isolation strings**.**

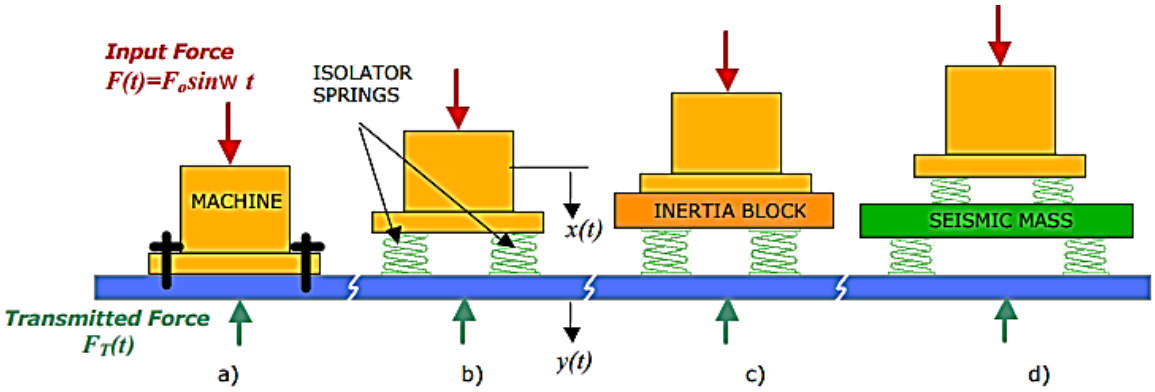

Figure 1. Complex vibration isolation systems.

In the past few years, various interesting efforts have been proposed for vibration positioning control systems. A very promising research domain is the magnetic levitation method [4] which dealt with a suspension method that enables an object to be suspended without any support except magnetic fields only. Related works in this area presented in [5], [6], [7], [8], [9], [10], [11], [12], [13], [14] and [15]. These works lacks investigation on damper parameter configuration for systems such as in Figure 1. This current study involves the analysis of a similar vibration isolation system with two geometrically orientated damping devices at ninety degrees to the parallel combination of a linear damper and spring.

Consequently, the objective of this study is to investigate the effect of the selected damper configuration for better performance and then design a nonlinear damping parameter for the system. In this context, a force-excited system with low amplitude excitation is considered here and the OFRF technique [16] is employed in the analysis and design of the nonlinear damping parameter for the vibration isolation system.

The paper is organized as follows: the process nonlinear model involving the damping force is presented in Section 2. The proposed Output Frequency Response Function Method is next developed in Section 3. The experimental deductions are presented in Section 4. Experimental Results (OFRF Model Analysis) are discussed in Section 5 and the conclusions are highlighted in Section 6.

2. Process Model Description

The system under investigation is shown in Figure 2. This represents the process model diagram. The horizontal damping elements have got linear characteristics with damping coefficients c_h but contribute a nonlinear effect due to its orientation.

It is integrated in a typical single degree-of-freedom (SDOF) vibration isolation system with a suspended mass, m and a parallel combination of two linear springs with each stiffness $\frac{k}{2}$. The orientation of the two horizontal auxiliary damping devices c_h is at a 90-degree inclination to the parallel linear spring and damper combination. The source of vibration (also the disturbing force excitation) is the input to the isolation system given as f_{in} while the force transmitted to the stiff foundation of the isolation system f_{out} is chosen as the system output.

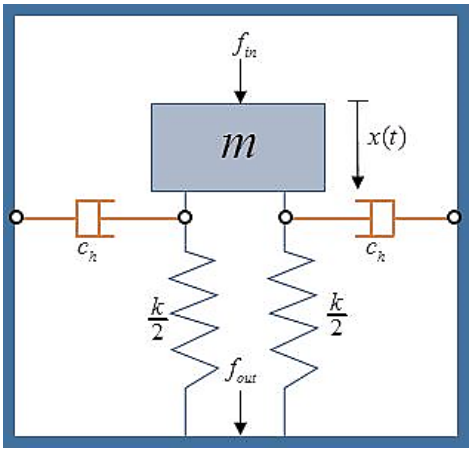

Figure 2: SDOF vibration isolation system with horizontal linear dampers.

The damping force due to the horizontal damper in the direction of the spring (towards the base), f_d is given by

$$f_d = \frac{c_h x^2}{(a^2 + x^2)} \dot{x} \tag{1}$$

Where a is the length of the damper, x is the resolved vertical displacement across the damper.

From Eq. (1), it is observed that the damping force strongly depends on the vertical displacement across the damper as well as its velocity in the vertical direction. Thus, the governing equation of Figure 2 becomes,

$$\left.\begin{aligned} m\ddot{x} + c_v\dot{x} + c_{eq}\dot{x} + kx &= f_{in} \\ f_{out} &= c_v\dot{x} + c_{eq}\dot{x} + kx \end{aligned}\right\} \tag{2}$$

where the equivalent resultant damping for both dampers in the vertical direction is

$$c_{eq} = \frac{2c_h x^2}{(a^2 + x^2)} \tag{3}$$

However, under low amplitude excitation and when $\left|\frac{x}{a}\right| < 0.2$, Eq. 3 can be approximated, as revealed in [3] to Eq. 4

$$c_{eq} = 2c_h \frac{x^2}{a^2} = \overline{c}_h x^2 \tag{4}$$

Assuming harmonic excitation for the disturbing force, $f_{in} = F_{in}sin(\omega t)$
Therefore, Eq. 2 can be written as

$$\left.\begin{aligned} m\ddot{x} + c_v\dot{x} + \overline{c}_h x^2\dot{x} + kx = F_{in}sin(\omega t) \\ f_{out} = c_v\dot{x} + \overline{c}_h x^2\dot{x} + kx \end{aligned}\right\} \quad (5)$$

In the next section, the OFRF method is briefly highlighted and subsequently employed in later sections for the analysis of Eq. 5.

3. Output Frequency Response Function Method

In this section, a brief discussion of the OFRF strategy is given. The output frequency response of a nonlinear dynamic system, as has been demonstrated in [17], can be expressed in a more explicit polynomial form revealing a relationship between the output spectrum and the parameters defining the system nonlinearities. This polynomial form is known as the OFRF of the system. This notion is valid for the class of nonlinear systems stable at zero equilibrium.

Assume the Volterra systems described by the subsequent differential equation

$$\sum_{m=1}^{M}\sum_{p=0}^{m}\sum_{k_1,\ldots k_{p+q}=0}^{K} c_{pq}(k_1,\ldots k_{p+q})\prod_{i=1}^{p}\frac{d^{k_i}y(t)}{dt^{k_i}}\prod_{i=p+1}^{p+q}\frac{d^{k_i}u(t)}{dt^{k_i}} = 0. \quad (6)$$

where $\frac{d^k y(t)}{dt^k}|_{k=0} = y(t)$ and $p+q=m$. M = maximum degree of nonlinearity, and K = maximum order of the derivative in terms of $y(t)$ and $u(t)$. The model parameters $c_{0,1}(\cdot)$ and $c_{1,0}(\cdot)$ are specified as linear parameters, equivalent to the model linear parameters i.e. $\frac{d^k y(t)}{dt^k}$ and $\frac{d^k u(t)}{dt^k}$ for $k = 0,1,\ldots,L$ and $c_{p,q}(\cdot)$, with $p+q \geq 2$, are specified as nonlinear parameters equivalent to the model nonlinear terms coefficients of the form $\prod_{i=1}^{p}\frac{d^{k_i}y(t)}{dt^{k_i}}\prod_{i=p+1}^{p+q}\frac{d^{k_i}u(t)}{dt^{k_i}}$ and $p+q$ is referred to as the nonlinear degree of the nonlinear parameter $c_{p,q}(\cdot)$. The OFRF of the system model in Eq. 6 can be represented by a polynomial function of the model parameters in the form

$$Y(j\omega) = \sum_{j_1=0}^{m_1}\cdots\sum_{j_{s_N}=0}^{m_{s_N}}\varphi_{j_1\cdots j_{s_N}}(j\omega)\lambda_1^{j_1}\cdots\lambda_{s_N}^{j_{s_N}} \quad (7)$$

where, $Y(j\omega)$ is the output frequency response of the model in Eq. 6, $\varphi_{j_1\cdots j_{s_N}}(j\omega)$ are complex-valued functions (OFRF coefficients) and $\lambda_1^{j_1}\cdots\lambda_{s_N}^{j_{s_N}}$ is a monomial function of model parameters of Eq. 6.
The structure of the OFRF, which can also be referred to as the monomials, is determined by using the algorithm given in Eq. 8

$$M_n = \left[\bigcup_{k_1,\ldots,k_n=0}^{K}[c_{0n}(k_1,\ldots,k_n)]\right]\bigcup\left[\bigcup_{q=1}^{n-1}\bigcup_{p=1}^{n-q}\bigcup_{k_1,\ldots,k_n=0}^{K}([c_{pq}(k_1,\ldots,k_{p+q})]\otimes M_{n-q,p})\right]\bigcup\left[\bigcup_{p=2}^{n}\bigcup_{k_1,\ldots,k_n=0}^{K}([c_{p0}(k_1,\ldots,k_{p+q})]\otimes M_{n,p})\right] \quad (8)$$

where $\otimes$ is the Kronecker product. The terms $M_{n,p}$, M_{n1} and M_1 are defined as in Eq. 9

$$M_{n,p} = \bigcup_{i=1}^{n-p+1}(M_i\otimes M_{n-i,p-1}),\ M_{n1} = M_n \text{ and } M_1 = [1] \quad (9)$$

The set of monomials as given in Eq. 8 can be expressed as

$$\Psi = \bigcup_{n=1}^{N} M_n \tag{10}$$

Therefore the OFRF representation of the system model in Eq. 6 can be written as

$$Y(j\omega) = \Psi \cdot \Phi(j\omega)^{\mathrm{T}} \tag{11}$$

where the set of complex-valued functions , $\Phi(j\omega) = \varphi_{j_1 \cdots j_{s_N}}(j\omega) = [\varphi_0(j\omega)\ \varphi_1(j\omega)\varphi_2(j\omega)\cdots\ \varphi_N(j\omega)]$

The OFRF method has been thoroughly studied in [16-18].

4. OFRF Model Deduction and Reprenstation

In this section, the OFRF representation of the model in Eq. 5 is obtained.The maximum order of derivative, $K = 2$ and maximum degree of nonlinearity in terms of $y(t)$, $M = 3$. Therefore, it can be deduced from Eq. 5 that $c_{10}(2) = m$, $c_{10}(1) = c_v$, $c_{30}(001) = \overline{c}_h$, $c_{10}(0) = k$, $c_{01}(0) = -1$ and all other parameters are zero. In this study, the nonlinear parameter $c_{30}(001) = \overline{c}_h$ is the parameter of interest.

4.1. Determination of Monominals

The set of monomials required to obtain the OFRF representation for Eq. 5 is determined using Eqs. 8 to 10. This yields the following

$$M_1 = [1],\ M_2 = 0,\ M_3 = [\overline{c}_h],\ M_4 = 0,\ M_5 = [\overline{c}_h^{\,2}],\ M_6 = 0, M_7 = [\overline{c}_h^{\,3}],\ M_8 = 0,\ M_9 = [\overline{c}_h^{\,4}],\ M_{10} = 0,\ M_{11} = [\overline{c}_h^{\,5}]$$

$$M_{12} = 0, M_{13} = [\overline{c}_h^{\,6}], M_{14} = 0, M_{15} = [\overline{c}_h^{\,7}]$$

Therefore, the set of monomials where $N = 15$ is obtained as

$$\Psi = \bigcup_{n=1}^{15} M_n = [1\ \overline{c}_h\ \overline{c}_h^2\ \overline{c}_h^3\ \overline{c}_h^4\ \overline{c}_h^5\ \overline{c}_h^6\ \overline{c}_h^7] \tag{12}$$

4.2. Determination of the frequency function vector

The frequency function vector $\Phi(j\omega)$ is determined applying the methods shown in [18]. Seven different values of the nonlinear damping parameter $\overline{c}_h$ are chosen. These are $\overline{c}_h = [0.02, 2, 4, 6, 8, 10]$ The values of $\overline{c}_h$ are used to obtain 7 corresponding time domain output responses and the Fast Fourier Transform of these responses are obtained at the excitation frequency of interest. The OFRF coefficient $\Phi(j\omega)$ is obtained using least squares thus

$$\Phi(j\omega) = (\Psi^T\Psi)^{-1}\Psi^T \cdot \begin{bmatrix} Y(j\omega)|_{\overline{c}_h(1)} \\ Y(j\omega)|_{\overline{c}_h(2)} \\ \vdots \\ Y(j\omega)|_{\overline{c}_h(7)} \end{bmatrix} \tag{13}$$

where,

$$\Psi = \begin{bmatrix} 1 & \overline{c}_h(1) & \cdots & \overline{c}_h^7(1) \\ 1 & \overline{c}_h(2) & \cdots & \overline{c}_h^7(2) \\ \vdots & \vdots & \ddots & \vdots \\ 1 & \overline{c}_h(7) & \cdots & \overline{c}_h^7(7) \end{bmatrix} \quad \text{and} \quad \Phi(j\omega) = [\varphi_0(j\omega),\ \varphi_1(j\omega), \varphi_2(j\omega),\ \varphi_3(j\omega)..., \varphi_6(j\omega), \varphi_7(j\omega)]$$

Therefore, the OFRF representation is given as

$$Y_{out}(j\omega) = \varphi_0(j\omega) + \bar{c}_h \cdot \varphi_1(j\omega) + \bar{c}_h^2 \cdot \varphi_2(j\omega) + \bar{c}_h^3 \cdot \varphi_3(j\omega) + \bar{c}_h^4 \cdot \varphi_4(j\omega) + \bar{c}_h^5 \cdot \varphi_5(j\omega) + \bar{c}_h^6 \cdot \varphi_6(j\omega) + \bar{c}_h^7 \cdot \varphi_7(j\omega) \quad (14)$$

where $Y_{out}(j\omega)$ is the output frequency response of the system and $\varphi_0(j\omega), \varphi_1(j\omega),...,\varphi_7(j\omega)$ are complex-valued functions of frequency. The unit of each term in Eq.(14) is dependent on the individual force measurement and this is the decibel (dB). For example, the unit of $\varphi_0(j\omega)$ is the dB but that of $\varphi_1(j\omega)$ is dBm^3 / Ns^3.

5. Experimental Results/OFRF Model Analysis

The system design was tested on the nonlinear laboratory system and validated by real-time experiments involving the parameters values in Table 1. In all cases, the desired output response and the damping parameters were obtained. The responses were exclusively combined in position-velocity space . OFRF parameters of stiffness, damping, and offset angle were derived from a linear spring-damper system based on the torque profile. The OFRF polynomial derived and shown in Eq. (14) was employed in the design of the nonlinear damping parameter c_h for any desired output response $Y_{out}(j\omega)$. This is done by solving the polynomial for any desired output spectrum.

Table 2 shows the nonlinear damping design parameter c_h for six (6) desired output response. The solution for the OFRF polynomial yields 7 roots which could be either real or complex conjugate pairs. But since the damping parameter c_h must be real and non-negative, therefore c_h becomes the minimum non-negative solution to Eq.(14).

Table 1: Nonlinear Design Damping Responses.

Desired output response $20*\log(\lvert Y_{out}(j\omega)\rvert)$ (dB)	Obtained damping parameter $c_h(Ns/m)$
0.05	9.02
2	7.43
4	6.61
6	5.27
10	4.34
15	2.82

The values of the estimated OFRF coefficients, $\varphi_0(j\omega), \varphi_1(j\omega),...,\varphi_6(j\omega),\varphi_7(j\omega)$ at $\omega_0 = 20$ rad/s are given in Table 2.

Table 2. Evaluated values of $\Phi(j\omega)$ at resonance, $\omega_0 = 20\text{rad/s}$.

$\varphi_0(j\omega)$	-14741.4219020124 + 23999.6275760504i
$\varphi_1(j\omega)$	-11.2971154619583 + 13.1530910243196i
$\varphi_2(j\omega)$	0.000268832644392276 - 0.000382587282664353i
$\varphi_3(j\omega)$	-6.54144424275934e-10 + 1.22984159088396e-09i
$\varphi_4(j\omega)$	-6.41388586667339e-14 + 8.37725539017663e-14i
$\varphi_5(j\omega)$	7.15790625782278e-19 - 9.53294974070743e-19i
$\varphi_6(j\omega)$	-2.78368911861619e-25 + 2.88830774209864e-25i
$\varphi_7(j\omega)$	-1.60629538056844e-29 + 2.20998387221361e-29i

A force transmissibility graph showing the system output spectrum of Eq. 5 using both numerical and the OFRF methods is plotted and shown in Figure. 3.

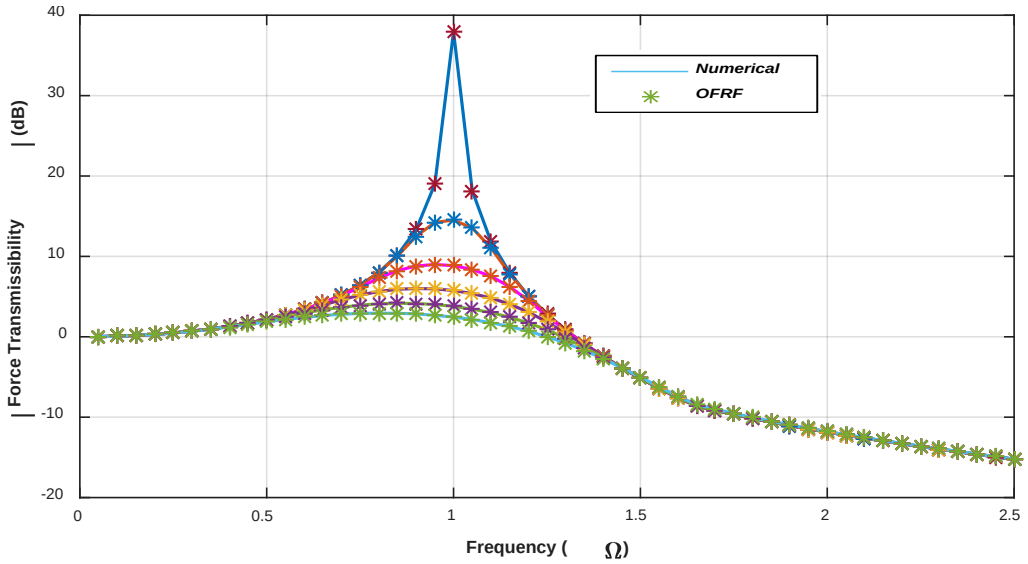

Figure 3: Force transmissibility against frequency for different values of $c_h = [0.02, 2, 4, 6, 8, 10]$ for both numerical (Solid line) and the OFRF methods (asterisks).

It is observed in Figure 3 that the force transmissibility of the vibration isolation system decreases at resonance ($\Omega = 1$) as the damping coefficient increases.

A surface plot of the force transmissibility is shown in Figure 4 showing the relationship between the force transmissibility of the isolation system, the damping coefficients and the excitation frequencies.

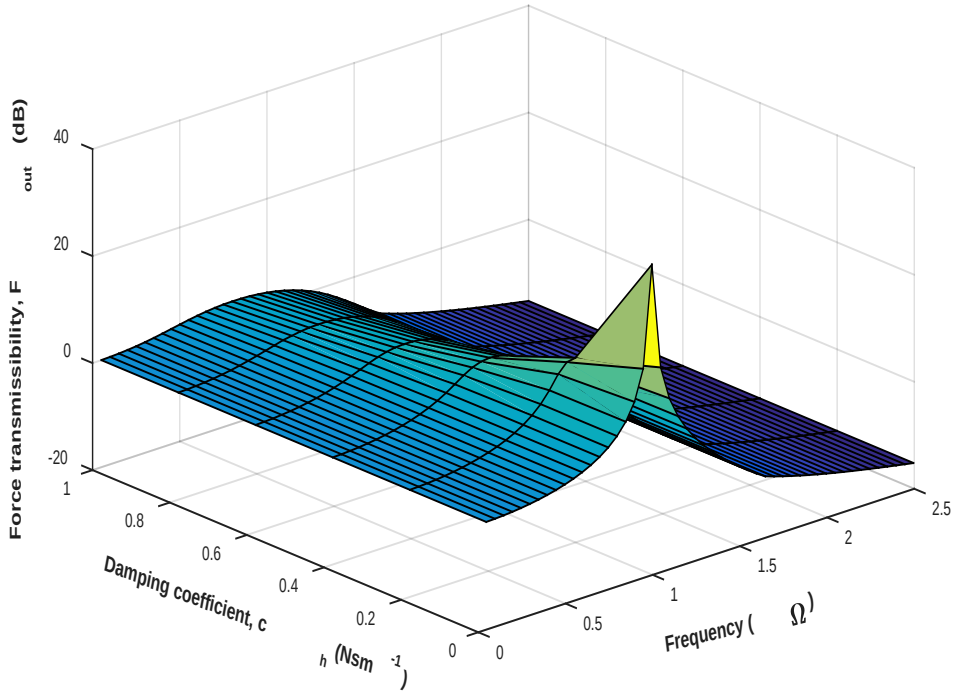

Figure 4: Force transmissibility against frequency for different values of $c_h = [0.02, 2, 4, 6, 8, 10]$

CONCLUSION

The paper has discussed and analyzed the characteristics of the vibration isolation system with dampers orientated perpendicularly (at 90 degrees) to the linear spring. It was been observed that the damping system contributes a nonlinear effect to the system dynamical response owing to its geometry. The OFRF process model was used in the analytical study of the isolation system. The OFRF polynomial of the system model was derived and subsequently used in the analysis. For a set of desired output responses, corresponding nonlinear damping parameters were designed using the OFRF representations. The effects of different excitations and damping parameters on the output response were also shown. Finally, a table showing the designed damping parameters for various desired output responses was presented based on real time experimental computations. The real-time experimental results prove that the OFRF structure discussed in this paper guarantees the improvement of vibration isolation. As shown in the previous section, the choice of the parameters of the design parameters in Table 1 has been carried out by conducting several experiments while aiming at the optimal values from the OFRF polynomial derived. Since Nonlinear auto regressive with eXegenous input (NARX) approach [19] is yet to be fully explored, future research will focus on alternative choice of OFRF parameters [20]. Its optimization will be explored and compared with Nonlinear auto regressive with eXegenous input (NARX) approach. This will involve optimal tuning using classical approaches, modern optimization algorithms and then, the combined approaches (classical and modern). Also, this work will implement control system design with PID adaptive fuzzy vibration isolation controllers. Moreover, we shall employ the Mamdani, Sugeno FIS, and Tsukamoto Fuzzy Inference Systems (FIS) while making comparisons with magnetic levitation system approaches for improved performance metrics.

Conflict of Interest

We declare that there is no conflict of intrest.

Acknowlegedement

This paper is an extended and revised version of a preliminary conference report that was presented in Nigercon 2017 at Federal University of Technology Owerri, Nigeria.

References

[1]. R., MarkusThier, R. Hainisch, G.chitter; integrated system and control design of a one DoF nano-metrology platform, Elseiver mechatronics, Vol.47.Pp. 88-96. 2017. https://doi.org/10.1016/j.mechatronics.2017.08.013

[2]. Linlin Li, Chun-Xia Li, Guoying Gu , Li-Min Zhu ; Positive acceleration, velocity and position feedback based damping control approach for piezo-actuated nano-positioning stages, Elseiver Mechatronics, Vol.47, 2017.Pp.97-104. https://doi.org/10.1016/j.mechatronics.2017.09.003.

[3]. B. Tang and M. J. Brennan. "A comparison of two nonlinear damping mechanisms in a vibration isolator." Journal of Sound and Vibration 332, No. 3, 2013: 510-520.

[4]. B. Tang and M. J. Brennan. "A comparison of the effects of nonlinear damping on the free vibration of a single-degree-of-freedom system." Journal of Vibration and Acoustics 134, no. 2, 2012: 024501.

[5]. C.-A. Bojan-Dragos, R.-E. Precup, M.L. Tomescu, S. Preitl, O.-M. Tanasoiu, S. Hergane; Proportional-Integral-Derivative Gain-Scheduling Control of a Magnetic Levitation System, International Journal of Computers Communications & Control, 12(5), 599-611, October 2017.

[6]. Shameli E., Khamesee M.B., Huissoon J.P.; Nonlinear controller design for a magnetic levitation device, Microsystem Technologies, 13(8), 831-835, 2007.

[7]. Wang B.; Liu G.-P.; Rees D.; Networked predictive control of magnetic levitation system, Proceedings of 2009 IEEE International Conference on Systems, Man and Cybernetics, San Antonio, TX, USA, 4100–4105, 2009.

[8]. Sakalli A., Kumbasar T., Yesil E., Hagras H,; Analysis of the performances of type- 1, self-tuning type-1 and interval type-2 fuzzy PID controllers on the magnetic levitation system, Proceedings of 2014 IEEE International Conference on Fuzzy Systems, Beijing, China, 1859-1866, 2014.

[9]. Zietkiewicz J. ; Constrained predictive control of a levitation system, Proceedings of 16th International Conference on Methods and Models in Automation and Robotics, Miedzyzdroje, Poland, 278-283, 2011.

[10]. Chauhan S., Nigam M.J.; Model predictive controller design and perturbation study for magnetic levitation system, Proceedings of 2014 IEEE Recent Advances in Engineering and Computational Sciences, Chandigarh, India, 1-6, 2014.

[11]. Pallav S., Pandey K., Laxmi V.; PID control of magnetic levitation system based on derivative filter, Proceedings of 2014 Annual International Conference on Emerging Research Areas: Magnetics, Machines and Drives, Kottayam, India, 1-5, 2014.

[12]. Huang Y.-W., Tung P.-C.; Design of a fuzzy gain scheduling controller having input saturation: a comparative study, Journal of Marine Science and Technology, 17(4), 249-256, 2009.

[13]. Elsodany N.M., Rezeka S.F., Maharem N.A. ; Adaptive PID control of a stepper motor driving a flexible rotor, Alexandria Engineering Journal, 50(2), 127-136, 2011.

[14]. Bianchi F.D., Sánchez Peña R.S. ; Interpolation for gain-scheduled control with guarantees, Automatica, 47(1), 239-243, 2011.

[15]. An S., Ma Y., Cao Z. ; Applying simple adaptive control to magnetic levitation system, Proceedings of 2nd International Conference on Intelligent Computation Technology and Automation, Changsha, Hunan, China, 1, 746-749, 2009.

[16]. Z.Q. Lang and S. A. Billings; Output frequency characteristics of nonlinear systems." International Journal of Control 64, no. 6. 1049-1067.

[17]. Z.Q. Lang, S. A. Billings, R. Yue, and J. Li.; Output frequency response function of nonlinear Volterra systems." Automatica 43, No. 5. 805-816.

[18]. H. Laalej, Z.Q. Lang, S. Daley, I. Zazas, S. A. Billings, and G. R. Tomlinson (2012); Application of nonlinear damping to vibration isolation: an experimental study." Nonlinear Dynamics 69, no. 1-2. 409-421.

[19]. Yunpeng Zhu and Z. Q. Lang, "Design of Nonlinear Systems in the Frequency Domain: An Output Frequency Response Function-Based Approach", In IEEE Transactions on Control Systems Technology, Volume: PP, Issue: 99, Pp.1-14, July 12, 2017.Digital Object Identifier 10.1109/TCST.2017.2716379. June 2017.

[20]. Diala Uchenna, K.C. Okafor, Lang Zi-Qiang, "Geometrical Non-linear Damper Design - A Frequency Based Approach", *In Proc.& IEEE Xplore- 3rd International Conference on Electro technology for National development*, (NIGERCON 2017), Federal University of Technology, Owerri, Nigeria. November 7-10, 2017.